Title

MRI-based screening for structural definition of eligibility in clinical DMOAD trials: Rapid OsteoArthritis MRI Eligibility Score (ROAMES)

Journal

Osteoarthritis and Cartilage, 28(1)

ISSN

1063-4584

Authors

Roemer, FW
Collins, J
Kwoh, CK
et al.

Publication Date

2020

DOI

10.1016/j.joca.2019.08.005

Peer reviewed

HHS Public Access

Author manuscript

Osteoarthritis Cartilage. Author manuscript; available in PMC 2021 January 01.

Published in final edited form as:

Osteoarthritis Cartilage. 2020 January ; 28(1): 71–81. doi:10.1016/j.joca.2019.08.005.

MRI-based screening for structural definition of eligibility in clinical DMOAD trials: Rapid OsteoArthritis MRI Eligibility Score (ROAMES)

Frank W. Roemer[1,2], **Jamie Collins**[3], **C. Kent Kwoh**[4], **Michael J. Hannon**[5], **Tuhina Neogi**[6], **David T. Felson**[6], **David J. Hunter**[7], **John A. Lynch**[8], **Ali Guermazi**[1]

[1]Quantitative Imaging Center, Department of Radiology, Boston University School of Medicine, FGH Building, 4th floor, 820 Harrison Avenue, Boston, MA 02118, USA

[2]Department of Radiology, Friedrich-Alexander University Erlangen-Nürnberg (FAU) and Universitätsklinikum Erlangen, Erlangen, Germany, Maximiliansplatz 3, 91054 Erlangen, Germany

[3]Orthopaedics and Arthritis Center of Outcomes Research, Brigham and Women's Hospital, Harvard Medical, School, 75 Francis Street, BTM Suite 5016 Boston, MA 02115 Boston, Massachusetts

[4]University of Arizona Arthritis Center & University of Arizona College of Medicine, 1501 N Campbell Ave, Tucson, AZ 85724, USA

[5]Pinney Associates, 201 N Craig St # 320, Pittsburgh, PA 15213, USA & Division of Rheumatology and Clinical Immunology, University of Pittsburgh School of Medicine, S700 Biomedical Science Tower, 3500 Terrace Street, Pittsburgh, PA 15261, USA (former affiliation at time of study)

Corresponding author and reprint requests: Frank W. Roemer, MD, Department of Radiology, University of Erlangen-Nuremberg, Maximiliansplatz 3, 91054 Erlangen, Germany, Tel +49 9131 8536065, Fax +49 9131 8536068, frank.roemer@uk-erlangen.de; Quantitative Imaging Center (QIC), Department of Radiology, Boston University School of Medicine, FGH Building, 4th floor, 820 Harrison Avenue, 02118 Boston, MA, Tel +1 617 414 3893 Fax +1 617 638 6616, froemer@bu.edu.

Authors contributions

(1) All authors were involved in the conception and design of the study, or acquisition of data, or analysis and interpretation of data.
(2) All authors contributed to drafting the article or revising it critically for important intellectual content.
(3) All authors gave their final approval of the manuscript to be submitted.

Additional contributions:

Analysis and interpretation of the data: FWR, JEC, CKK, DJH, DTF, TN, MJH, JL, AG
Drafting of the article: FWR, JEC, CKK, DJH, DTF, TN, MJH, JL, AG
Provision of study materials or patients: FWR; AG, JEC
Statistical expertise: JEC, MJH
Obtaining of funding: n/a
Collection and assembly of data: FWR; AG
Responsibility for the integrity of the work as a whole, from inception to finished article, is taken by F. Roemer, MD.

Conflict of interests

FWR is shareholder of Boston Imaging Core Lab. (BICL),LLC.
CKK is consultant to EMD Serono, Thusane, Express Scripts, Regulus, GSK, Regeneron, Fidia, Taiwan Liposome Company.
TN is consultant to Pfizer, EMD Merck Serono, Novartis.
DJH is consultant to Merck Serono, Pfizer, Tissuegene, TLCBio.
MH received an institutional grant by the NIH and is consultant to EMD Serono.
JEC is consultant to Boston Imaging Core Lab (BICL),LLC.
AG has received consultancies, speaking fees, and/or honoraria from Sanofi-Aventis, Merck Serono, and TissuGene and is President and shareholder of Boston Imaging Core Lab (BICL), LLC a company providing image assessment services.
DTF and JL have no conflict to declare.

[6]Boston University School of Medicine, Section of Rheumatology, 650 Albany Street, Suite X-20, Boston, MA, 02118, USA

[7]Department of Rheumatology, Royal North Shore Hospital and Institute of Bone and Joint Research, Kolling Institute, University of Sydney, Pacific Hwy, St Leonards, NSW 2065, Australia

[8]Department of Epidemiology and Biostatistics, University of California San Francisco, 550 16th St, San Francisco, CA 94158, USA

Abstract

Purpose: Our aim was to introduce a simplified MRI instrument, Rapid OsteoArthritis MRI Eligibility Score (ROAMES), for defining structural eligibility of patients for inclusion in disease-modifying osteoarthritis drug trials using a tri-compartmental anatomic approach that enables stratification of knees into different structural phenotypes and includes diagnoses of exclusion. We also aimed to define overlap between phenotypes and determine reliability.

Methods: 50 knees from the Foundation for National Institutes of Health Osteoarthritis Biomarkers study, a nested case-control study within the Osteoarthritis Initiative, were selected within pre-defined definitions of phenotypes as either inflammatory, subchondral bone, meniscus/cartilage, atrophic or hypertrophic. A focused scoring instrument was developed covering cartilage, meniscal damage, inflammation and osteophytes. Diagnoses of exclusion were meniscal root tears, osteonecrosis, subchondral insufficiency fracture, tumors, malignant marrow infiltration and acute traumatic changes. Reliability was determined using weighted kappa statistics. Descriptive statistics were used for determining concordance between the a priori phenotypic definition and ROAMES and overlap between phenotypes.

Results: ROAMES identified 43 of 50 (86%) pre-defined phenotypes correctly. Of the 50 participants, 27 (54%) had no additional phenotypes other than the pre-defined phenotype. 18 (36%) had one and 5 (10%) had two additional phenotypes. None had three or four additional phenotypes. All features of ROAMES showed almost perfect agreement. One case with osteonecrosis and one with a tumor were detected.

Conclusions: ROAMES is able to screen and stratify potentially eligible knees into different structural phenotypes and record relevant diagnoses of exclusion. Reliability of the instrument showed almost perfect agreement.

Keywords

MRI; osteoarthritis; eligibility; clinical trial

Introduction

Osteoarthritis (OA) is the most common type of arthritis and a leading cause of pain and disability among adults[1]. Although a number of potential disease-modifying molecules have been investigated in recent years, there is still no pharmacological agent approved by regulatory agencies as a disease-modifying OA drug (DMOAD)[2–6].

Imaging has an important role in determining structural disease severity and potential suitability of patients recruited to DMOAD trials. Radiographic structural disease severity is defined by the Kellgren-Lawrence (K-L) scale, a composite measure reflecting osteophyte presence and joint space narrowing[7]. While several variations of the K-L scale exist[8], knees with K-L grades 2 (definite osteophytes) and 3 (definite joint space narrowing) are commonly considered eligible for inclusion. Knees with a K-L grade of 0 or 1 are considered not to have structural OA, and thus, are excluded from participating in DMOAD trials[9]. However, OA knees commonly have heterogeneous structural joint damage that cannot be visualized by radiography[9,10]. MRI tissue alterations have been observed in a large majority of knees with normal radiographs (i.e. K-L grade 0) suggesting that radiography lacks sensitivity for detection of early OA structural changes[11], although the clinical significance of some of these alterations has yet to be confirmed. In addition, researchers are increasingly suggesting that there are several phenotypes or subpopulations in OA that are characterized by distinct clinical manifestations of disease, by certain laboratory parameters, biochemical markers, and/or imaging findings[12–14]. While MRI-based phenotypic characterization of large cohort data is not available to date[15], it has been suggested that there may be three main structural phenotypes in OA, i.e. meniscus/cartilage, subchondral bone and inflammation[16–18]. These may progress differently and may represent distinct tissue targets for DMOAD approaches[6,19]. In addition, an atrophic (extended cartilage loss with small osteophytes) and hypertrophic phenotype (large osteophytes with minor cartilage damage) have been described with both being rare[20,21]. However, it should also be noted that more than one pathogenetic mechanism may be involved in the same patient to varying degrees during different phases of the disease and that one phenotype seldom exists in isolation. Further, these structural phenotypes may be accompanied by varied clinical manifestations.

In addition, several entities have come into focus in recent years that are perceived to be potentially detrimental to the joint, are a reflection of systemic disease such as malignancy or are considered risk factors for rapid disease progression or joint collapse and thus, considered exclusionary in clinical DMOAD or symptom-relieving trials[14]. While in general these entities are considered uncommon, none of these are detectable by radiography or only at late stages.

Given the shortcomings of radiography as a screening tool in DMOAD trials, MRI could be considered an alternative to define eligibility criteria for structural parameters to classify potential study participants into various structural phenotypes and to detect potential diagnoses of exclusion. However, until now, MRI has been perceived as a tool that is too complex and expensive to be applied in large scale endeavors such as eligibility screening. Reasons for this perception are primarily cost-related based on lengthy image acquisition and complex assessment of the acquired images. While established MRI scoring systems have shown validity in an epidemiologic context and have been applied in a longitudinal fashion, these are typically too complex to be applied in a large-scale screening effort and also do not include potential diagnoses of exclusion. However, recent advances in MRI technology have markedly decreased image acquisition times[22–24] and focused image assessment may help overcome such perceived hurdles.

The aim of our study is to introduce a simplified MRI assessment instrument, the Rapid OsteoArthritis MRI Eligibility Score (ROAMES), using a tri-compartmental anatomic approach that is able to stratify knees into different structural phenotypes reflecting potential target tissues in regard to the mechanism of action of a specific DMOAD. In addition, we aimed to include diagnoses of exclusion not commonly covered by established assessment instruments and to determine the reliability of that instrument.

Methods

Sample Selection

Cases were selected from the Foundation for National Institutes of Health Osteoarthritis Biomarkers Consortium (FNIH) study a nested case-control study within the larger Osteoarthritis Initiative (OAI) study[19]. In brief, the OAI is a multicenter prospective observational cohort study of knee OA (https://oai.nih.gov) that enrolled 4796 participants aged 45–79 years at four clinical centers. Details of the OAI inclusionary and exclusionary criteria have been published[25].

Eligible participants for the FNIH study were those with at least one knee with a K-L grade of 1–3 at baseline. A pre-determined number of index knees was selected with cases (n = 406) having radiographic and/or pain progression at 48 months compared to the baseline visit. Controls (n = 194) were knee osteoarthritis subjects who had neither radiographic or pain progression[19]. For this current exercise and the purpose of developing the ROAMES instrument, 50 knees were selected from subsamples of the FNIH cohort that fulfilled the a priori definitions of one of five distinct structural phenotypes (10 knees for each phenotype) as described below and was based on publicly available semiquantitative assessments according to the MRI Osteoarthritis Knee Score (MOAKS)[26] system (readings performed by two radiologists, AG and FWR, with 20 and 17 years of experience in standardized MRI assessment of knee OA) at baseline. Case selection was performed regardless of potential overlap between phenotypes. The FNIH cohort was used as it is representing a sample comparable to common clinical trial inclusion criteria with knees having mild (K-L grade 1 or 2) to moderate (K-L grade 3) structural OA with symptoms and offers the possibility to evaluate patterns of progression. The sample size was chosen to ensure reasonable precision in the estimate of agreement statistics, such as the Kappa and overall agreement. More specifically, a sample size of 50 provides the following 95% confidence intervals: for a point estimate of 80% agreement, 66% to 90%; for a point estimate of 90% agreement, 78% to 97%.

Knee MRI acquisition

MRI of both knees was performed on identical 3 T systems (Siemens Trio, Erlangen, Germany) at the four OAI clinical sites. MRIs were acquired with a dedicated quadrature transmit/receive knee coil including a coronal intermediate-weighted (IW) two-dimensional (2D) turbo spin-echo, a sagittal three-dimensional (3D) dual echo at steady state (DESS) sequence with additional coronal and axial reformations, and a sagittal IW fat-suppressed turbo spin-echo sequence. Additional parameters of the full OAI pulse sequence protocol

and the sequence parameters have been published in detail[27]. All of these sequences were used for image assessment.

A priori phenotypic definition used for sample selection

According to the baseline FNIH MOAKS assessments five phenotypes were defined and used for selection of the sample: Inflammatory, meniscus/cartilage, subchondral bone, atrophic and hypertrophic. Currently, structural radiography-based screening for DMOAD trials only takes into account the tibiofemoral joint due to the traditional focus on the medial tibiofemoral compartment, the *a priori* definitions for the ROAMES sample also included structural pathology in the tibiofemoral joint only. Details of the a priori definitions that were the basis for knee selection for the ROAMES sample are presented in Appendix 1.

Description of ROAMES

The aim of this simplified scoring instrument is stratification into phenotypes and identification of joint diagnoses of exclusion. To achieve these goals a compartmental simplified coding of maximum grades is used differentiating the patellofemoral, the medial tibiofemoral (MTFJ) and the lateral tibiofemoral joint (LTFJ) while current semi-quantitative systems use a strict multi-subregional approach[28,26].

Cartilage: Based on a simplified WORMS grading a compartmental coding for the MTFJ, LTFJ and patello-femoral joint is performed. Maximum scores based on WORMS- or MOAKS-defined subregions (both are identical) are recorded. WORMS was used primarily as the basis for iteration instead of MOAKS as WORMS suggests a simpler scaling in regard to ordinal grading. The following grades are assigned: Grade 0 = normal cartilage surface; Grade 1 = maximum grade in compartment is a focal defect (i.e. WORMS 2 and 2.5); Grade 2 = maximum grade in compartment is superficial diffuse damage (i.e. WORMS 3 and 4); Grade 3 = maximum grade in compartment is diffuse full thickness damage (i.e. WORMS 5 and 6). Combined lesions (diffuse superficial plus small full thickness component) grades 2.1 and 3.1 in MOAKS will be categorized as 2 and 3 in ROAMES. For example, if one out of five subregions in the MTFJ exhibits a maximum cartilage grade of 3, the grades of the other four subregions will be ignored and 3 will be recorded as the compartmental score.

Bone Marrow Lesions (BMLs): In alignment with cartilage assessment BMLs are scored in the same WORMS-/MOAKS-subregions and only the maximum grade will be recorded as the compartmental score. Scores are assigned as described previously in MOAKS. Percentage of the volume of subregion that is representing ill-defined or cystic BML is graded as Grade 0 = none, Grade 1 <33%, grade 2 = 33–66% and grade 3 >66% of that subregion. The maximum score for a specific compartment will be recorded.

Osteophytes: The same locations as in MOAKS are applied in ROAMES for osteophyte scoring but only the largest osteophyte per compartment is recorded. Ordinal grading is performed aligned with MOAKS from 0–3 where Grade 0 = none, Grade 1 = small, Grade 2 = medium and Grade 3 = large. Osteophytes are scored in identical fashion to the MOAKS system.

Meniscus: For meniscal assessment only the maximum grade in the anterior horn, the body and the posterior horn are recorded resulting in one score for the medial and one score for the lateral meniscus. Scores are assigned as follows: Grade 0 = normal/signal; Grade 1 = simple horizontal-oblique tear; Grade 2 = all other tears; Grade 3 = any maceration/ substance loss; Grade 4 = posterior root tear. In addition, medial and lateral extrusion is assessed as described for the modified WORMS system: Grade 0 = normal; Grade 1 = less than 50%; Grade 2 = more than 50% of extrusion in the coronal planes assessed on the slice where the tibial spines are largest.

Inflammation: The features of Hoffa- and effusion-synovitis are scored in identical fashion as described for MOAKS. Hoffa-synovitis is scored on the sagittal intermediate fat suppressed sequence based on the degree of hyperintensity in Hoffa's fat pad: Grade 0= normal; Grade 1 = mild, Grade 2 = moderate, Grade 3 = severe. Effusion-synovitis is assessed based on the amount of capsular distension from 0–3 with Grade 0 = physiologic amount; Grade 1 = small; Grade 2 = medium; Grade 3 = large.

Diagnoses of exclusion: Additional diagnoses of exclusion are recorded in dichotomized fashion as present or absent. These include posterior meniscal root tears, subchondral insufficiency fractures, osteonecrosis, malignant bone marrow infiltration, solid tumors, and traumatic fracture or bone bruise. Figure 1 presents these diagnoses in illustrative and exemplary fashion.

The compartmental subdivision of ROAMES is shown in Figure 2. Representative image examples for the different phenotypes are presented in Figure 3.

ROAMES Assessment

Readings were performed by the same two radiologists who read the FNIH sample (AG, FWR). Prior the image assessment a calibration exercise of 4 hours was performed on 25 knee MRIs with pre-defined phenotypes (5 for each phenotype) from the FNIH dataset that were not used for the final readings. Both readers read the entire dataset of 50 knee MRIs. One radiologist (FWR) re-scored all MRIs in random order for all ROAMES features after a 4-week interval to determine intra-reader reliability. Image interpretation was performed blinded to clinical information using digital imaging software (eFilm Workstation, Version 4.2.0, Merge Healthcare, Milwaukee, Wisconsin).

Definition of phenotypes based on ROAMES

The following phenotypes were defined according to the ROAMES system reflecting the definitions of the a priori stratification based on MOAKS readings.

- Inflammatory: As described above for the a priori definition a maximum grade of 3 of either Hoffa- or effusion-synovitis and at least grade 2 in the respective other feature were required to fulfill the definition of inflammatory phenotype.
- Meniscus/cartilage: Presence of a meniscus score of at least ROAMES grade 3 (i.e. any type of meniscal substance loss/maceration) in the medial and/or lateral compartment and at least grade 1 (any type of tear) in the other compartment,

respectively, and presence of cartilage damage grades 2.1, 2.2, 3.2 or 3.3 according to MOAKS.

- Subchondral bone: Subregional BML size of grade 3 in at least one of three knee compartments.
- Atrophic: Osteophytes ≤ 1 in all locations of the TFJ and cartilage damage of grade 3 in at least one MOAKS subregion of one or both compartments of the TFJ.
- Hypertrophic: At least one osteophyte grade 3 in the medial TFJ and/or lateral TFJ and/or PFJ; cartilage damage not more than grade 1 in any subregion of the same compartment of the TFJ.

Analytic approach

Weighted kappa statistics were applied to determine inter- and intra-observer reliability of the parameters scored in ROAMES. The performance of ROAMES regarding the identification of predefined phenotypes according to MOAKS was determined describing the percentages of correctly identified cases for total sample and per phenotype. We present exact binomial confidence intervals for the percentages. In addition, a descriptive overview of additional phenotypes and overlap was calculated. All analyses were conducted in SAS 9.4 (SAS Institute, Cary NC).

Results

Mean age of the participants was 62 years, 60 % of the participants were women, average BMI was 31.2 kg/m2 (SD ± 4.6), mean medial minimum joint space width was 3.63 mm SD ± 1.35 mm). Regarding radiographic disease severity 1 knee had a K-L grade of 1, 24 knees a K-L grade of 2 and 25 knees had a K-L grade of 3. These demographic characteristic are comparable to the overall FNIH sample[19]. Of the 50 participants included, 25 had radiographic and pain progression, four exhibited radiographic progression but not pain progression, five had pain progression but not radiographic progression and 16 had neither radiographic progression nor pain progression. Demographic details for each phenotype group included are presented in Appendix 2. Weighted kappa values for intra-rater reliability were 0.99 for BMLs, 0.98 for cartilage, 0.99 for meniscus, and 0.98 for osteophytes. For inter-rater reliability the weighted kappa values were 0.97 for BMLs, 0.97 for cartilage, 0.98 for meniscus, and 0.96 for osteophytes.

ROAMES was able to identify 10 of 10 (100%, 95% Confidence Interval (CI): (69%, 100%)) cases with an inflammatory phenotype, 10 of 10 (100%, 95% CI: (69%, 100%)) cases with a meniscus/cartilage phenotype, 9 of 10 (90%, 95% CI: (56%, 100%)) with a bone phenotype, 8 of 10 (80%, 95% CI: (44%, 97%)) with a hypertrophic phenotype and 6 of 10 (60%, 95% CI: (26%, 88%)) with an atrophic phenotype. Altogether, ROAMES identified 43 of 50 (86%, 95% CI: (73%, 94%)) phenotypes correctly.

Each phenotype represented 20% of the sample and thus 40 knees (80%) were primarily not defined as that specific phenotype but could nonetheless fulfill the a priori definition of a

specific phenotype (e.g. 10 knees were pre-defined as inflammatory but nonetheless knees within the 40 other knees with a different phenotype could still fulfill the inflammatory definition). Of the non-predetermined 40 remaining phenotype cases 5 additional cases had an inflammatory phenotype according to ROAMES, 2 additional had a meniscus/cartilage phenotype, 13 additional had a bone phenotype, 2 additional had a hypertrophic phenotype and 6 additional had an atrophic phenotype. A detailed overview of these results is presented in Table 1.

Of the 50 knees, 27 (54%) had no additional phenotypes other than the one they were initially assigned. 18 (36%) had one additional phenotype and 5 (10%) had 2 additional phenotypes. None of the cases had 3 or 4 additional phenotypes. Appendix 3 presents an overview of phenotypic overlap and the number of additional phenotypes on a case basis.

The atrophic cases were the least likely to have an additional phenotype (80% had no additional phenotypes) and the inflammatory cases were the most likely (30% had no additional phenotypes).

All features of ROAMES showed almost perfect inter and intra-reader agreement according to weighted kappa values as shown in detail in Table 2.

In regard to diagnoses of exclusion one case exhibited a likely diagnosis of diffuse-type giant cell tumor of the tendon sheath (dGCTTS), and one knee showed an epiphyseal osteonecrosis identified by both readers.

While not part of study aims and not systematically recorded, ROAMES scoring that involved electronic coding of 19 features and anatomical assignments took on average 10–15 min per knee.

Discussion

We have introduced a simplified MRI scoring instrument for knee OA - ROAMES - that allows stratification of potential candidates to be included in DMOAD trials into five different phenotypes and can be used by experienced readers with excellent reliability. In addition, the instrument includes evaluation of diagnoses of exclusion that are commonly considered contraindications for inclusion and are only detectable by MRI.

Reasons for failure of DMOAD trials in recent years are complex but include X-ray based eligibility screening[6,14,16]. X-ray is only able to depict osseous changes and is not able to show OA-related tissue changes other than osteophytes, joint space narrowing, sclerosis, cysts and attrition - features that are commonly not considered treatment targets. Other shortcomings of radiography include challenges in reproducibility regarding positioning, which affects semi-quantitative as well as quantitative assessment[29]. Another relevant drawback of radiography in eligibility screening is the inability to detect diagnoses that may increase risk for joint collapse or fast progression regardless of potential DMOAD treatment. Thus, MRI seems to be an alternative for eligibility screening. MRI is capable of showing all joint tissues and is able to provide a detailed phenotypic characterization, including tissues that may be responsible for the pain experience in OA. Finally, MRI is able to screen for

subjects at risk for mentioned non-favorable diagnoses of exclusion. Commonly perceived hurdles in the application of MRI to eligibility assessment may be overcome as a result of technological advances and focused image assessment by tools such as ROAMES. While established whole-joint scoring instruments have shown validity in an epidemiologic context and are sensitive to change over time, these are too time-consuming and costly for application in a large-scale screening context (e.g., more than 100 knees for a single time-point MOAKS score)[26,28]. In addition, these established tools do not systematically cover diagnoses of exclusion that are relevant in a screening effort. Advances in imaging technology have enabled marked acceleration of image acquisition that may potentially reduce imaging time to a fraction of previous acquisition times, which will decrease associated acquisition costs significantly[22–24]. These advances include parallel imaging or improvements in 3D turbo spin echo (TSE) imaging that now allow for acquisition of triplanar MRI of the knee with fat-suppressed fluid sensitive contrast in less than 5 min. The current exercise used the OAI dataset for phenotypic characterization, which is based on conventional image acquisition with about 20 min duration for the five sequences used for the current assessment. However, in the past we showed that semiquantitative assessment of knee OA can be reliably performed using 3D TSE MRI (acquired in 5 min)[30]. Future work will likely show feasibility of ROAMES application to 2D or 3D MRI datasets acquired in 5–7 minutes. ROAMES uses standard fluid-sensitive fat-suppressed clinical sequences that are rarely affected by artifacts or resolution issues as these sequences are robust regarding artifacts and highly standardized.

We have differentiated five structural phenotypes in our exercise namely the inflammatory, meniscus/cartilage, subchondral bone, atrophic and hypertrophic phenotypes. The inflammatory phenotype is characterized by marked synovitis and /or joint effusion. Synovial activation in OA is thought to be a secondary phenomenon related to cartilage deterioration, and there is evidence that synovitis plays a role in the progression of cartilage loss in knee OA[18]. Several molecules have been investigated in recent years that are targeting primarily the inflammatory manifestations of OA such as IL-1, TNF-α and iNOS inhibitors[31–33]. The cartilage/meniscal phenotype exhibits meniscal damage and/or meniscal extrusion associated with severe cartilage loss on MRI. We know that meniscal pathology plays a role in predicting cartilage loss and BMLs in the tibiofemoral compartments including meniscal extrusion[34,35]. Pharmacologic meniscal repair is currently not available and whether a DMOAD may be able to restore cartilage in light of altered biomechanics due to severe meniscal damage and particularly maceration remains to be shown. Future work will have to show whether severe meniscal substance loss may be an exclusionary criterion for DMOAD inclusion. The subchondral bone phenotype was defined in the current study by large BMLs. BMLs are defined on MRI as non-cystic subchondral areas of ill-defined hyperintensity on fluid sensitive fat suppressed MRI sequences that are frequently seen in conjunction with cartilage damage in the same region[36]. BMLs play an important role in predicting structural progression[37,38]. Fluctuation and even resolution of BMLs has been observed and change of symptoms in subjects with knee OA has been associated with change of BMLs in the same direction[39,40]. Thus, BMLs have become a treatment target for novel therapeutic approaches[5,41]. Based on the presence or absence of osteophytes, a hypertrophic or atrophic OA phenotype was defined in addition. A cross-sectional

community-based study evaluating different phenotypes of knee OA on MRI demonstrated that severe cartilage damage in the knee is commonly associated with large osteophytes[20]. An atrophic OA phenotype has been described exhibiting no or only tiny osteophytes yet marked cartilage loss[20]. A recent study based within the MOST cohort surprisingly showed that the atrophic phenotype of knee OA was associated with a decreased likelihood of progression of JSN and cartilage loss compared to the non-atrophic knee OA phenotype[21]. Additional work will have to show the relevance of these two specific phenotypes in light of DMOAD trial inclusion. We acknowledge that structural characterization based on imaging findings is only one aspect to define criteria for clinical trial inclusion, demographic and clinical parameters are similarly relevant and include factors such as age, pain, function, BMI, alignment, etc.

In addition, there are diagnoses that should ideally be excluded at screening as these will not be amenable to a DMOAD but will show a negative outcome regardless of potential treatment of OA. Tumors of the knee joint, both benign and malignant, although rare, may be observed as incidental findings in screening efforts. Diffuse infiltration of the bone marrow may be observed in several hematologic and oncologic diseases and although rare in general may be encountered in an OA sample as an incidental finding. Subchondral insufficiency fractures of the knee are difficult to detect and may have an unpredictable course due to delayed diagnosis and lack of standard treatment approaches[42,43]. Posterior root tears of the medial meniscus result in instability of the knee and are associated with more severe meniscal extrusion and more cases of osteonecrosis compared with horizontal tears[44]. It is likely that the impaired biomechanics based on root tears will over-ride potential DMOAD effects[45].

We used an expert reading approach to assess MRIs in simplified semiquantitative fashion compared to commonly used tools such as WORMS or MOAKS. We acknowledge that training and calibration are important to achieve adequate agreement in scoring between readers. Scoring per knee took between 10 and 15 min and thus, seems feasible for assessment of a large number of potential knees in screening efforts. Centralized reading in a multicenter setting requires logistical efforts, however, comparable feasibility has been shown in clinical trials before and the advantages may potentially outweigh some minor time delays[46,47]. One may argue that machine learning approaches are potentially able to screen MRI data in order to define structural characteristics for patient inclusion. However, at present a detailed evaluation of relevant joint pathology that will have impact on patient recruitment seems only be feasible by expert assessment. To date none of the algorithms has shown to be able to differentiate types of meniscal tears including those that will have major impact on outcomes such as root tears. In addition the vast differential diagnosis of bone marrow changes including artifacts requires profound insight into imaging techniques and musculo-skeletal disease pathologies. Tools to extract cartilage in a fully automated and reliable manner from 3D sequences are only being developed[48,49]. For such reasons it is likely that expert assessment will be the current most feasible approach for MRI-based screening endeavors in DMOAD trials. The instrument presented showed excellent reliability after training and applied by experienced readers. Due to the simplification of the scoring system superior agreement compared with more complex MRI reading systems could be achieved.

Limitations of our study include the small sample size with only 10 knees per distinct phenotype and overlap between phenotypes that needs to be characterized further. We have observed a proportion of knees that exhibited more than one but none more than three concomitant phenotypes. Dell'Isola et al., in their characterization of the FNIH cohort, used a wider spectrum of definitions and incorporated MRI data to define an inflammatory phenotype and as a secondary criterion for a malalignment subgroup[50]. In that analysis overlap was described for 20% of the cases. The relevance of overlapping structural phentoypes as also seen in our sample needs to be defined for each treatment target and may differ between studies. A larger sample is necessary to assess diagnostic performance of ROAMES using common metrics like sensitivity, specificity and area under the curve (AUC) as well as expanded analysis of phenotype overlap and its relevance, in a similar fashion to Dell'Isola et al. for the entire FNIH dataset[50]. We acknowledge that there may be different cut-offs in regard to defining specific phenotypes and ours were arbitrarily chosen based on clinical experience and potential relevance. If other definitions may be more appropriate needs to be defined further. In addition, future work will have to show rates of progression for each distinct phenotype and how these differ. Finally, the relevance of the rare atrophic and hypertrophic phenotypes for patient inclusion to clinical trials remains unclear, particularly as the atrophic and meniscus/cartilage phenotype are overlapping.

In summary, we introduced a focused rapid scoring instrument, ROAMES that is able to screen and stratify potentially eligible knees into different structural phenotypes and record relevant diagnoses of exclusion much faster than commonly used semiquantitative scoring schemes. Diagnoses of exclusion are not covered by published whole-organ approaches. Reliability of this instrument is excellent and currently perceived hurdles such as costs and access to MRI system in a multicenter setting may be overcome by rapid image acquisition using standard clinical sequences. Potentially, the suggested phenotypic stratification may result in more targeted trial populations and will hopefully decrease the numbers of participants included in DMOAD trials that should not be included considering the potential specific mode of action of a given pharmacological compound.

Supplementary Material

Refer to Web version on PubMed Central for supplementary material.

Acknowledgments

We would like to thank the OAI participants, OAI investigators, OAI clinical and technical staff, the OAI coordinating center and the OAI funders for providing this unique public data base. The study and data acquisition was funded by the OAI, a public-private partnership comprised of five contracts (N01-AR-2–2258; N01-AR-2–2259; N01-AR-2–2260; N01-AR-2–2261; N01-AR-2–2262) funded by the National Institutes of Health, a branch of the Department of Health and Human Services, and conducted by the OAI Study Investigators. Private funding partners of the OAI include Merck Research Laboratories; Novartis Pharmaceuticals Corporation, GlaxoSmithKline; and Pfizer, Inc. Private sector funding for the OAI is managed by the Foundation for the National Institutes of Health. The sponsors were not involved in the design and conduct of this particular study, in the analysis and interpretation of the data, and in the preparation, review, or approval of the manuscript. TN was supported by NIH K24 AR070892.

Funding and role of the funding source

No funding was received for this study.

References

1. Hunter DJ, Schofield D, Callander E. The individual and socioeconomic impact of osteoarthritis. Nat Rev Rheumatol 2014;10:437–41. [PubMed: 24662640]
2. Karsdal MA, Byrjalsen I, Henriksen K, Riis BJ, Lau EM, Arnold M, et al. The effect of oral salmon calcitonin delivered with 5-CNAC on bone and cartilage degradation in osteoarthritic patients: a 14-day randomized study. Osteoarthritis Cartilage 2010;18:150–9. [PubMed: 19747581]
3. Spector TD, Conaghan PG, Buckland-Wright JC, Garnero P, Cline GA, Beary JF, et al. Effect of risedronate on joint structure and symptoms of knee osteoarthritis: results of the BRISK randomized, controlled trial [ISRCTN01928173]. Arthritis Res Ther 2005;7:R625–33. [PubMed: 15899049]
4. Alexandersen P, Karsdal MA, Byrjalsen I, Christiansen C. Strontium ranelate effect in postmenopausal women with different clinical levels of osteoarthritis. Climacteric 2011;14:236–43. [PubMed: 20726814]
5. Reginster JY, Badurski J, Bellamy N, Bensen W, Chapurlat R, Chevalier X, et al. Efficacy and safety of strontium ranelate in the treatment of knee osteoarthritis: results of a double-blind, randomised placebo-controlled trial. Ann Rheum Dis 2013;72:179–86. [PubMed: 23117245]
6. Hunter DJ. Pharmacologic therapy for osteoarthritis--the era of disease modification. Nat Rev Rheumatol 2011;7:13–22. [PubMed: 21079644]
7. Kellgren JH, Lawrence JS. Radiological assessment of osteo-arthrosis. Ann Rheum Dis 1957;16:494–502. [PubMed: 13498604]
8. Schiphof D, Boers M, Bierma-Zeinstra SM. Differences in descriptions of Kellgren and Lawrence grades of knee osteoarthritis. Ann Rheum Dis 2008;67:1034–6. [PubMed: 18198197]
9. Guermazi A, Hunter DJ, Roemer FW. Plain radiography and magnetic resonance imaging diagnostics in osteoarthritis: validated staging and scoring. J Bone Joint Surg Am 2009;91 Suppl 1:54–62. [PubMed: 19182026]
10. Guermazi A, Roemer FW, Felson DT, Brandt KD. Motion for debate: osteoarthritis clinical trials have not identified efficacious therapies because traditional imaging outcome measures are inadequate. Arthritis Rheum 2013;65:2748–58. [PubMed: 23861096]
11. Guermazi A, Niu J, Hayashi D, Roemer FW, Englund M, Neogi T, et al. Prevalence of abnormalities in knees detected by MRI in adults without knee osteoarthritis: population based observational study (Framingham Osteoarthritis Study). BMJ 2012;345:e5339. [PubMed: 22932918]
12. Karsdal MA, Bihlet A, Byrjalsen I, Alexandersen P, Ladel C, Michaels M, et al. OA phenotypes, rather than disease stage, drive structural progression--identification of structural progressors from 2 phase III randomized clinical studies with symptomatic knee OA. Osteoarthritis Cartilage 2015;23:550–8. [PubMed: 25576879]
13. Mobasheri A The future of osteoarthritis therapeutics: targeted pharmacological therapy. Curr Rheumatol Rep 2013;15:364. [PubMed: 24061701]
14. Roemer FW, Kwoh CK, Hayashi D, Felson DT, Guermazi A. The role of radiography and MRI for eligibility assessment in DMOAD trials of knee OA. Nat Rev Rheumatol 2018;14:372–80. [PubMed: 29752462]
15. Deveza LA, Melo L, Yamato TP, Mills K, Ravi V, Hunter DJ. Knee osteoarthritis phenotypes and their relevance for outcomes: a systematic review. Osteoarthritis Cartilage 2017;25:1926–41. [PubMed: 28847624]
16. Oo WM, Yu SP, Daniel MS, Hunter DJ. Disease-modifying drugs in osteoarthritis: current understanding and future therapeutics. Expert Opin Emerg Drugs 2018;23:331–47. [PubMed: 30415584]
17. Felson DT. Osteoarthritis as a disease of mechanics. Osteoarthritis Cartilage 2013;21:10–5. [PubMed: 23041436]
18. Berenbaum F Osteoarthritis as an inflammatory disease (osteoarthritis is not osteoarthrosis!). Osteoarthritis Cartilage 2013;21:16–21. [PubMed: 23194896]
19. Collins JE, Losina E, Nevitt MC, Roemer FW, Guermazi A, Lynch JA, et al. Semiquantitative Imaging Biomarkers of Knee Osteoarthritis Progression: Data From the Foundation for the

National Institutes of Health Osteoarthritis Biomarkers Consortium. Arthritis Rheumatol 2016;68:2422–31. [PubMed: 27111771]

20. Roemer FW, Guermazi A, Niu J, Zhang Y, Mohr A, Felson DT. Prevalence of magnetic resonance imaging-defined atrophic and hypertrophic phenotypes of knee osteoarthritis in a population-based cohort. Arthritis Rheum 2012;64:429–37. [PubMed: 22094921]
21. Crema MD, Felson DT, Guermazi A, Nevitt MC, Niu J, Lynch JA, et al. Is the atrophic phenotype of tibiofemoral osteoarthritis associated with faster progression of disease? The MOST study. Osteoarthritis Cartilage 2017;25:1647–53. [PubMed: 28606556]
22. Fritz J, Fritz B, Thawait GG, Meyer H, Gilson WD, Raithel E. Three-Dimensional CAIPIRINHA SPACE TSE for 5-Minute High-Resolution MRI of the Knee. Invest Radiol 2016;51:609–17. [PubMed: 27187045]
23. Fritz J, Fritz B, Zhang J, Thawait GK, Joshi DH, Pan L, et al. Simultaneous Multislice Accelerated Turbo Spin Echo Magnetic Resonance Imaging: Comparison and Combination With In-Plane Parallel Imaging Acceleration for High-Resolution Magnetic Resonance Imaging of the Knee. Invest Radiol 2017;52:529–37. [PubMed: 28430716]
24. Altahawi FF, Blount KJ, Morley NP, Raithel E, Omar IM. Comparing an accelerated 3D fast spin-echo sequence (CS-SPACE) for knee 3-T magnetic resonance imaging with traditional 3D fast spin-echo (SPACE) and routine 2D sequences. Skeletal Radiol 2017;46:7–15. [PubMed: 27744578]
25. Nevitt MC, Felson DT, Lester G. The Osteoarthritis Initiative: protocol for the cohort study. p. 19–20. URL: http://oai.epi-ucsf.org/datarelease/docs/StudyDesignProtocol.pdf. Accessed February 20,2019
26. Hunter DJ, Guermazi A, Lo GH, Grainger AJ, Conaghan PG, Boudreau RM, et al. Evolution of semi-quantitative whole joint assessment of knee OA: MOAKS (MRI Osteoarthritis Knee Score). Osteoarthritis Cartilage 2011;19:990–1002. [PubMed: 21645627]
27. Peterfy CG, Schneider E, Nevitt M. The osteoarthritis initiative: report on the design rationale for the magnetic resonance imaging protocol for the knee. Osteoarthritis Cartilage 2008;16:1433–41. [PubMed: 18786841]
28. Peterfy CG, Guermazi A, Zaim S, Tirman PF, Miaux Y, White D, et al. Whole-Organ Magnetic Resonance Imaging Score (WORMS) of the knee in osteoarthritis. Osteoarthritis Cartilage 2004;12:177–90. [PubMed: 14972335]
29. Kinds MB, Vincken KL, Hoppinga TN, Bleys RL, Viergever MA, Marijnissen AC, et al. Influence of variation in semiflexed knee positioning during image acquisition on separate quantitative radiographic parameters of osteoarthritis, measured by Knee Images Digital Analysis. Osteoarthritis Cartilage 2012;20:997–1003. [PubMed: 22542633]
30. Crema MD, Nogueira-Barbosa MH, Roemer FW, Marra MD, Niu J, Chagas-Neto FA, et al. Three-dimensional turbo spin-echo magnetic resonance imaging (MRI) and semiquantitative assessment of knee osteoarthritis: comparison with two-dimensional routine MRI. Osteoarthritis Cartilage 2013;21:428–33. [PubMed: 23274102]
31. Chevalier X, Goupille P, Beaulieu AD, Burch FX, Bensen WG, Conrozier T, et al. Intraarticular injection of anakinra in osteoarthritis of the knee: a multicenter, randomized, double-blind, placebo-controlled study. Arthritis Rheum 2009;61:344–52. [PubMed: 19248129]
32. Verbruggen G, Wittoek R, Vander Cruyssen B, Elewaut D. Tumour necrosis factor blockade for the treatment of erosive osteoarthritis of the interphalangeal finger joints: a double blind, randomised trial on structure modification. Ann Rheum Dis 2012;71:891–8. [PubMed: 22128078]
33. Hellio le Graverand MP, Clemmer RS, Redifer P, Brunell RM, Hayes CW, Brandt KD, et al. A 2-year randomised, double-blind, placebo-controlled, multicentre study of oral selective iNOS inhibitor, cindunistat (SD-6010), in patients with symptomatic osteoarthritis of the knee. Ann Rheum Dis 2013;72:187–95. [PubMed: 23144445]
34. Englund M, Guermazi A, Roemer FW, Yang M, Zhang Y, Nevitt MC, et al. Meniscal pathology on MRI increases the risk for both incident and enlarging subchondral bone marrow lesions of the knee: the MOST Study. Ann Rheum Dis 2010;69:1796–802. [PubMed: 20421344]

35. Roemer FW, Felson DT, Wang K, Crema MD, Neogi T, Zhang Y, et al. Co-localisation of non-cartilaginous articular pathology increases risk of cartilage loss in the tibiofemoral joint--the MOST study. Ann Rheum Dis 2013;72:942–8. [PubMed: 22956600]
36. Roemer FW, Frobell R, Hunter DJ, Crema MD, Fischer W, Bohndorf K, et al. MRI-detected subchondral bone marrow signal alterations of the knee joint: terminology, imaging appearance, relevance and radiological differential diagnosis. Osteoarthritis Cartilage 2009;17:1115–31. [PubMed: 19358902]
37. Roemer FW, Zhang Y, Niu J, Lynch JA, Crema MD, Marra MD, et al. Tibiofemoral joint osteoarthritis: risk factors for MR-depicted fast cartilage loss over a 30-month period in the multicenter osteoarthritis study. Radiology 2009;252:772–80. [PubMed: 19635831]
38. Felson DT, McLaughlin S, Goggins J, LaValley MP, Gale ME, Totterman S, et al. Bone marrow edema and its relation to progression of knee osteoarthritis. Ann Intern Med 2003;139:330–6. [PubMed: 12965941]
39. Zhang Y, Nevitt M, Niu J, Lewis C, Torner J, Guermazi A, et al. Fluctuation of knee pain and changes in bone marrow lesions, effusions, and synovitis on magnetic resonance imaging. Arthritis Rheum 2011;63:691–9. [PubMed: 21360498]
40. Roemer FW, Guermazi A, Javaid MK, Lynch JA, Niu J, Zhang Y, et al. Change in MRI-Detected subchondral bone marrow lesions is associated with cartilage loss - the MOST study A longitudinal multicenter study of knee osteoarthritis. Ann Rheum Dis 2009;68:1461–5. [PubMed: 18829615]
41. Pelletier JP, Roubille C, Raynauld JP, Abram F, Dorais M, Delorme P, et al. Disease-modifying effect of strontium ranelate in a subset of patients from the Phase III knee osteoarthritis study SEKOIA using quantitative MRI: reduction in bone marrow lesions protects against cartilage loss. Ann Rheum Dis 2015;74:422–9. [PubMed: 24297379]
42. Wilmot AS, Ruutiainen AT, Bakhru PT, Schweitzer ME, Shabshin N. Subchondral insufficiency fracture of the knee: A recognizable associated soft tissue edema pattern and a similar distribution among men and women. Eur J Radiol 2016;85:2096–103. [PubMed: 27776664]
43. Jose J, Pasquotti G, Smith MK, Gupta A, Lesniak BP, Kaplan LD. Subchondral insufficiency fractures of the knee: review of imaging findings. Acta Radiol 2015;56:714–9. [PubMed: 24919465]
44. Sung JH, Ha JK, Lee DW, Seo WY, Kim JG. Meniscal extrusion and spontaneous osteonecrosis with root tear of medial meniscus: comparison with horizontal tear. Arthroscopy 2013;29:726–32. [PubMed: 23395469]
45. Marzo JM, Gurske-DePerio J. Effects of medial meniscus posterior horn avulsion and repair on tibiofemoral contact area and peak contact pressure with clinical implications. Am J Sports Med 2009;37:124–9. [PubMed: 18815238]
46. Guermazi A, Hunter DJ, Li L, Benichou O, Eckstein F, Kwoh CK, et al. Different thresholds for detecting osteophytes and joint space narrowing exist between the site investigators and the centralized reader in a multicenter knee osteoarthritis study--data from the Osteoarthritis Initiative. Skeletal Radiol 2012;41:179–86. [PubMed: 21479521]
47. Lohmander LS, Hellot S, Dreher D, Krantz EF, Kruger DS, Guermazi A, et al. Intraarticular sprifermin (recombinant human fibroblast growth factor 18) in knee osteoarthritis: a randomized, double-blind, placebo-controlled trial. Arthritis Rheumatol 2014;66:1820–31. [PubMed: 24740822]
48. Lee JG, Gumus S, Moon CH, Kwoh CK, Bae KT. Fully automated segmentation of cartilage from the MR images of knee using a multi-atlas and local structural analysis method. Med Phys 2014;41:092303. [PubMed: 25186408]
49. Ambellan F, Tack A, Ehlke M, Zachow S. Automated segmentation of knee bone and cartilage combining statistical shape knowledge and convolutional neural networks: Data from the Osteoarthritis Initiative. Med Image Anal 2019;52:109–18. [PubMed: 30529224]
50. Dell'Isola A, Steultjens M. Classification of patients with knee osteoarthritis in clinical phenotypes: Data from the osteoarthritis initiative. PLoS One 2018 1 12;13(1):e0191045. [PubMed: 29329325]

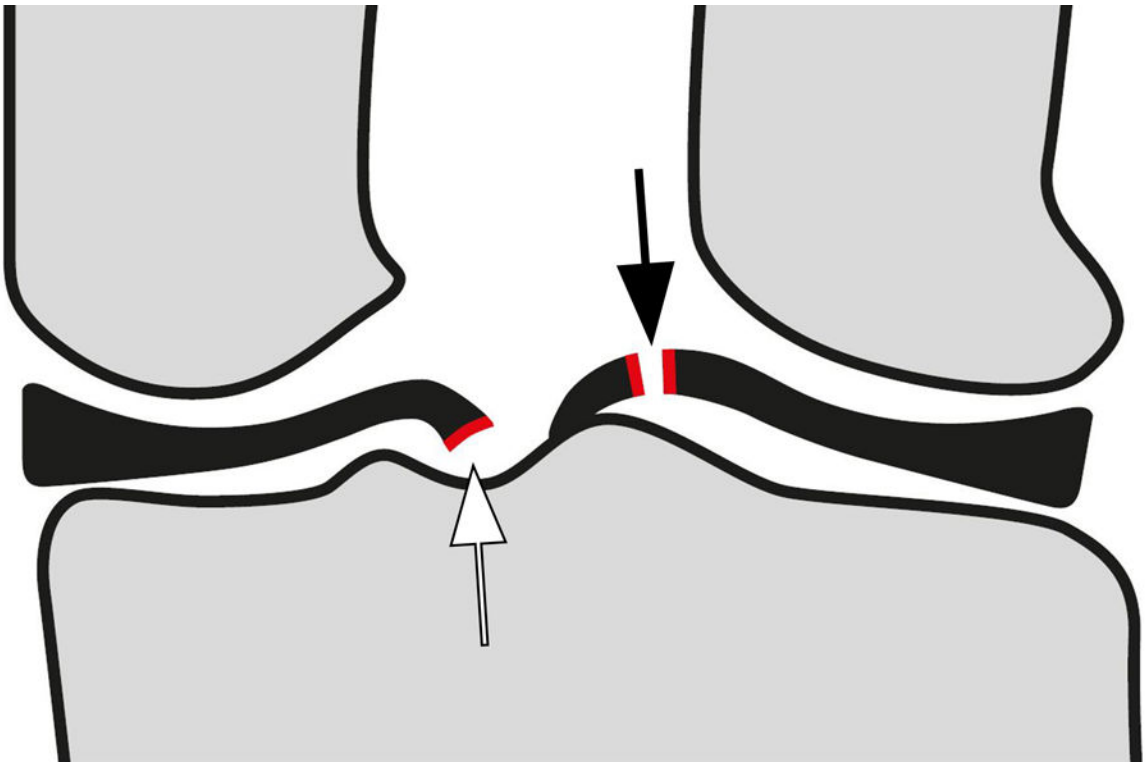

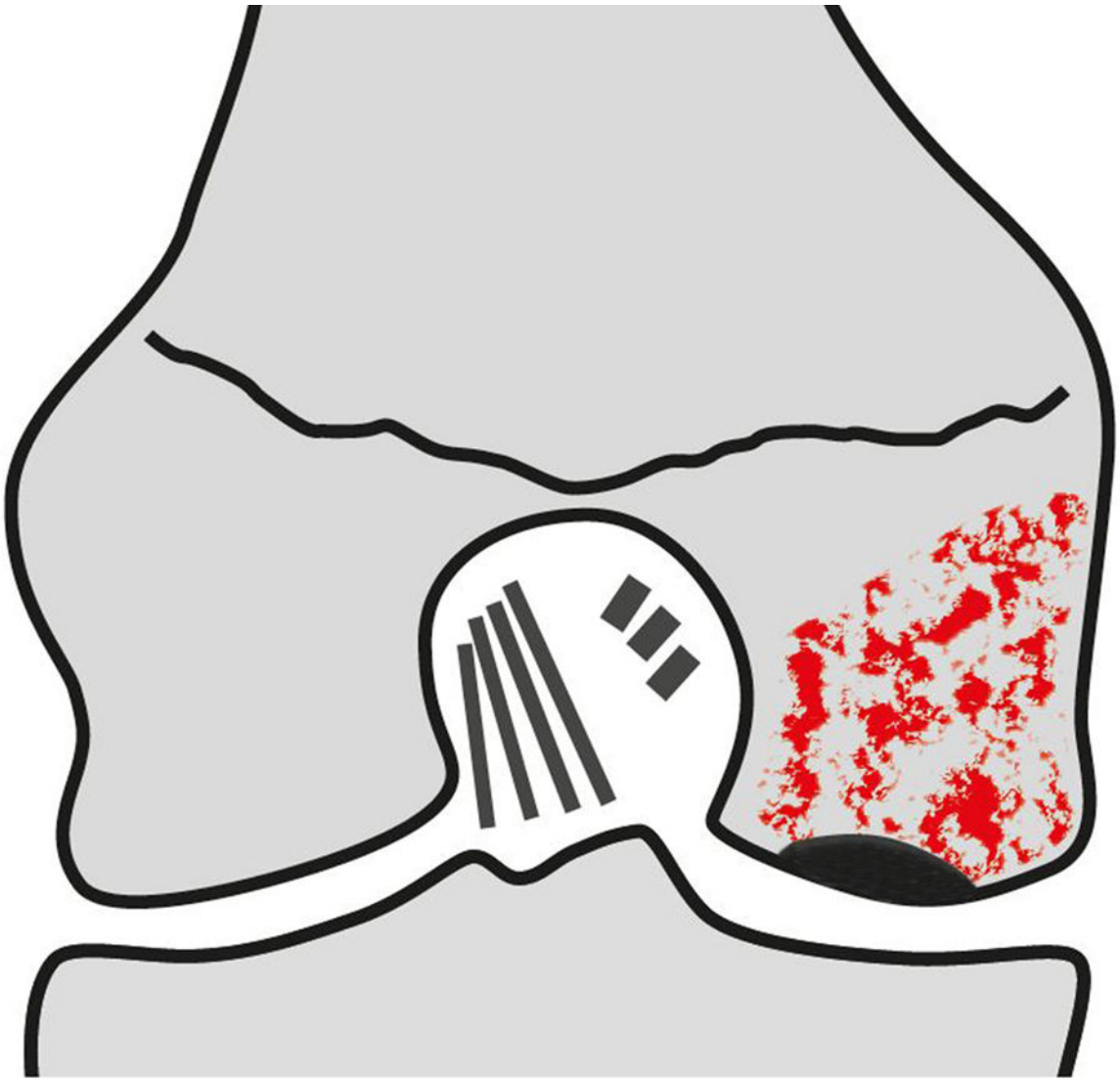

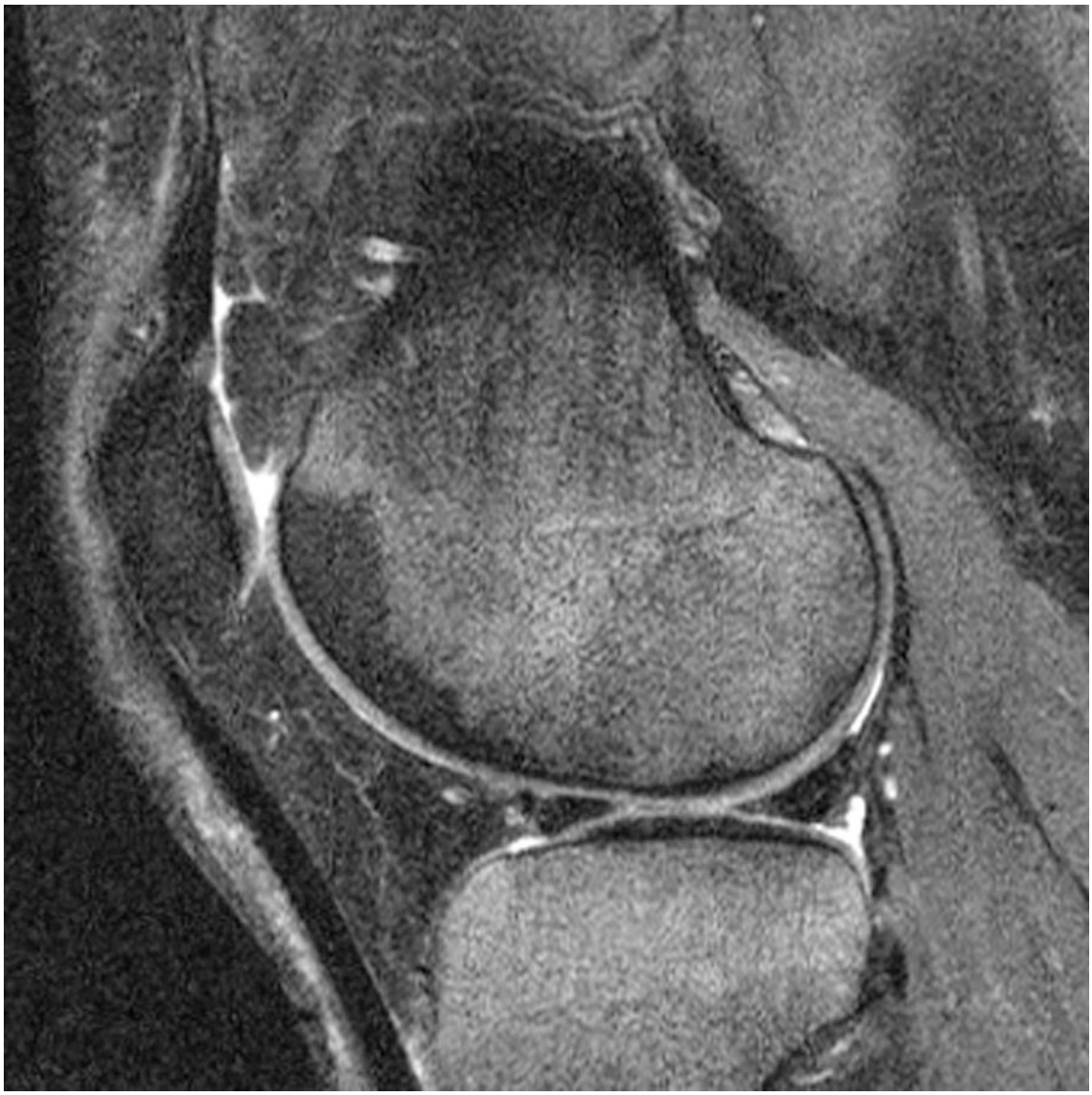

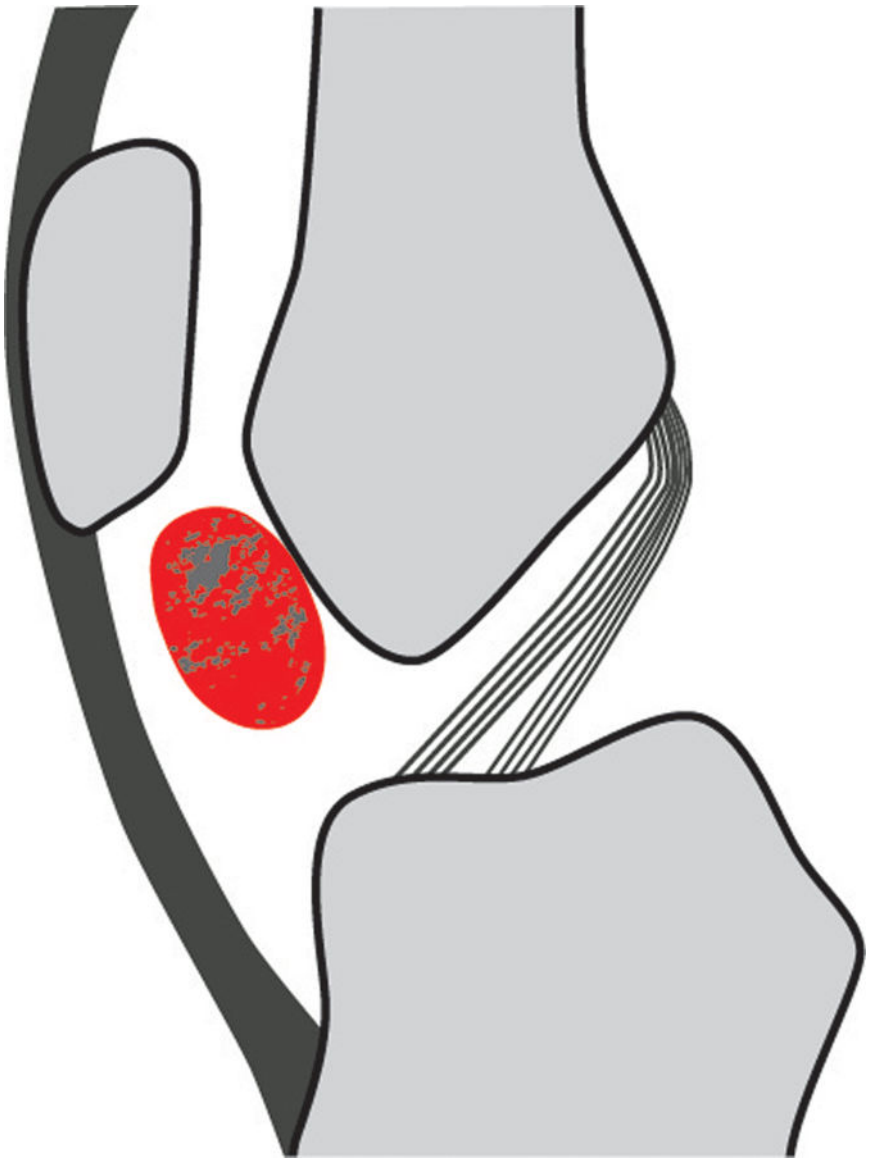

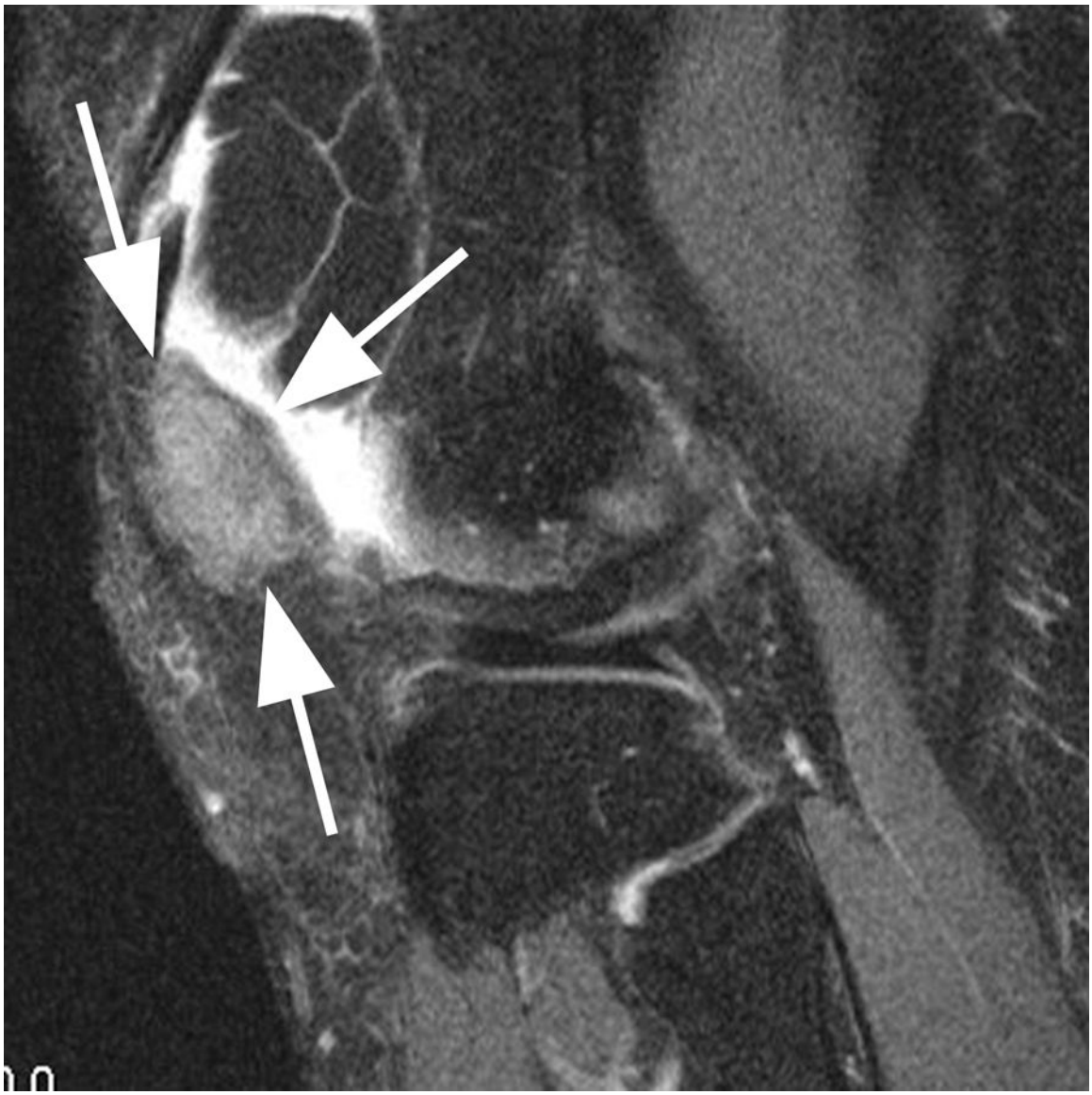

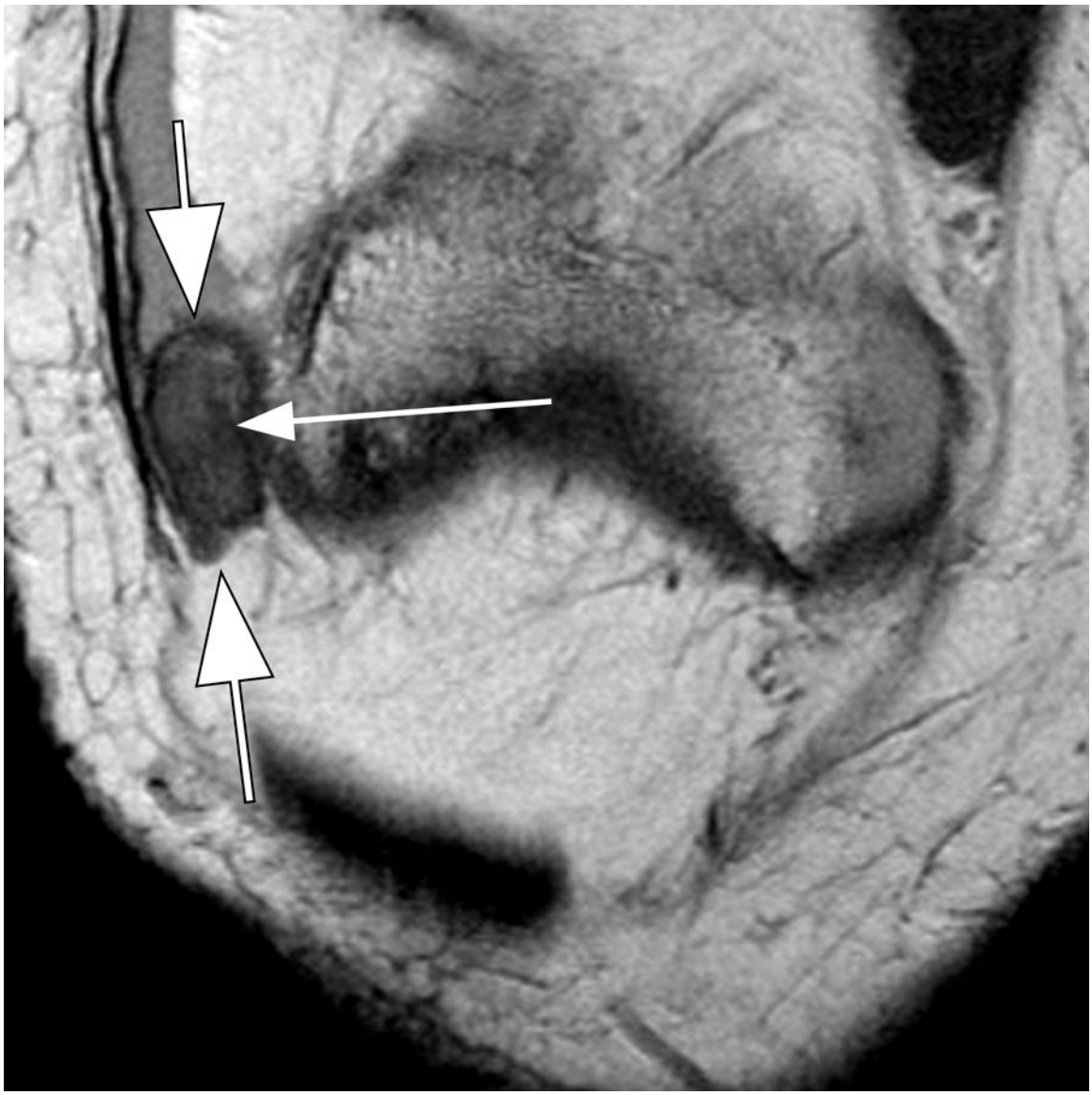

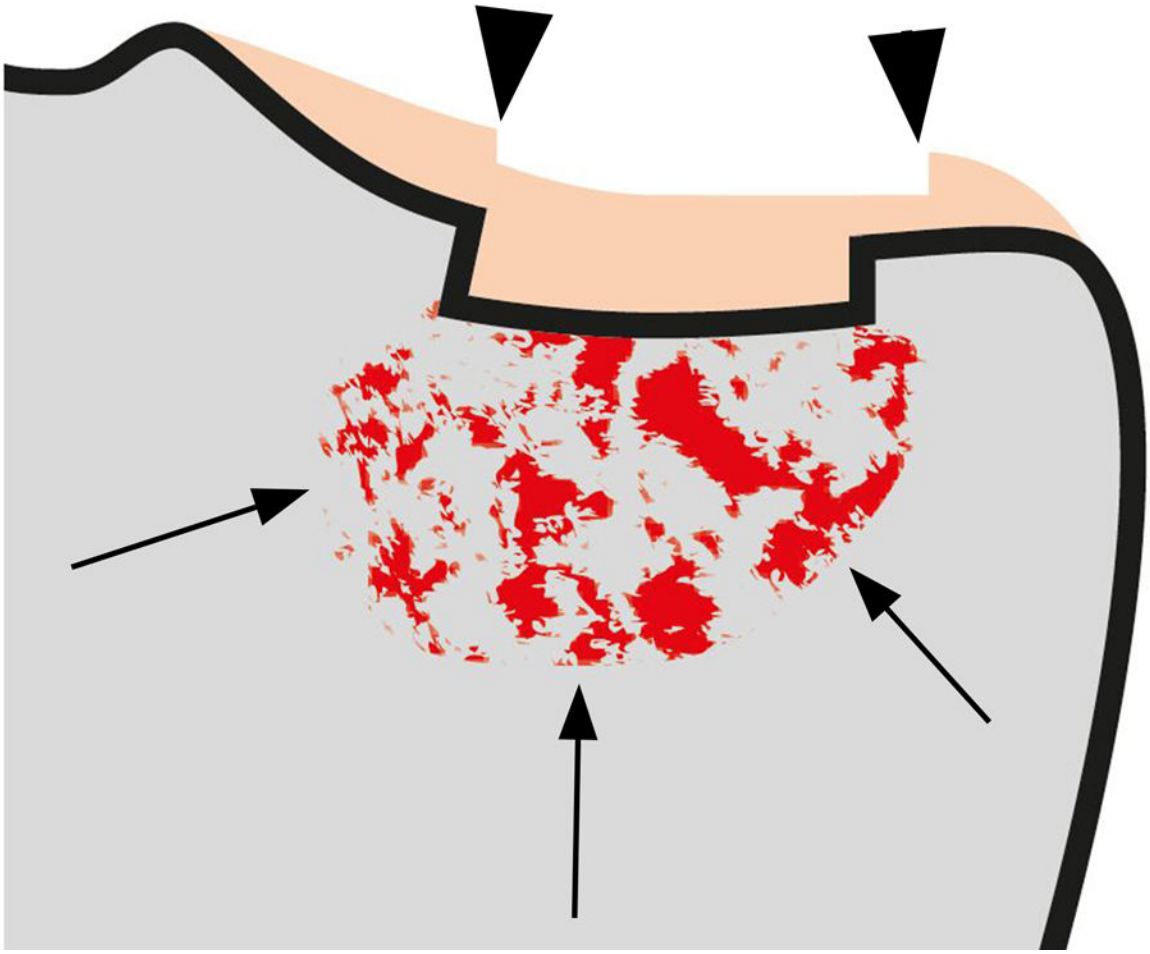

Figure 1.

Diagnoses of Exclusion: A. Posterior meniscal root tears are defined by avulsion of the meniscal ligamentous root (white arrow) or by complete radial tears close to the tibial attachment of the meniscus (black arrow). These tears result in biomechanical alterations comparable to a complete meniscectomy and may lead to rapid cartilage loss and potentially joint collapse. B. Coronal intermediate-weighted fat-suppressed image shows a medial posterior root tear (arrow). C. Subchondral insufficiency fractures are defined by a hypointense fracture line adjacent to the subchondral plate surrounded by a large area of bone marrow edema. Subchondral insufficiency fractures may heal or may progress to articular osteochondral defects and joint collapse. D. Coronal intermediate-weighted image depicts a subchondral insufficiency fracture (arrow) with a large area of surrounding bone marrow edema. E. Bone infarct or avascular necrosis is defined by a serpiginous area of hyperintensity on fluid sensitive fat-suppressed sequences and a fat-equivalent center. These are commonly observed in conjunction with systemic disease or steroid therapy and may increase the risk of joint collapse particularly when in an epiphyseal subchondral location. F.

A large area of epiphyseal osteonecrosis is shown on this sagittal intermediate weighted fat-suppressed image. Arrows point to the demarcation line. Infarcts are characterized by a serpiginous hyperintense demarcation and a fat-equivalent center. In addition, there is an area of cartilage delamination at the posterior lateral femur (short arrow). This fragment is at high risk of detachment and developing into an osteochondral defect and subsequent possible joint collapse. G. Diffuse cellular bone marrow infiltration due to malignancy such as lymphoma or leukemia may be diagnosed by MRI and needs to be differentiated from red marrow reconversion in anemia. The latter is not observed in an epiphyseal location while cellular infiltration is. H. Sagittal intermediate-weighted fat-suppressed image shows diffuse marrow infiltration due to acute lymphatic leukemia. Cellular infiltrations characterized by diffuse hyperintensity on fluid-sensitive sequences including the epiphyses as well as metaphyses. I. Pigmented villo-nodular synovitis (PVNS) or diffuse-type giant cell tumor of the tendon sheath (dGCTTS) are solid, benign tumors of the articular cavity that need surgical treatment and tend to recur. These are commonly observed adjacent to Hoffa’s fat pad in the anterior knee compartment as shown here. J. Sagittal intermediate-weighted image shows an oval-shaped lesion of intermediate signal intensity (arrows) in the anterior compartment of the knee joint. K. Coronal intermediate-weighted image shows the same lesion in the lateral gutter of the patello-femoral joint (short arrows). Long arrow points to focal intralesional hypointensities characteristic of representing hemosiderin deposits. L. Acute articular damage may result in a spectrum of morphologic findings from subchondral contusions to chondral flake fractures or osteochondral depression, as shown in this example. Commonly traumatic bone marrow edema (also called contusion) is seen in a subchondral location (arrows). In addition, there is a sharply delineated chondral depression (arrowheads) and also a contour deformity of the subchondral plate in this illustration. M. Sagittal intermediate-weighted fat-suppressed image shows a large bone contusion (i.e. traumatic bone marrow lesion) in the posterior lateral tibia. In addition, there is an osteochondral depression with disruption of the subchondral plate (arrow).”

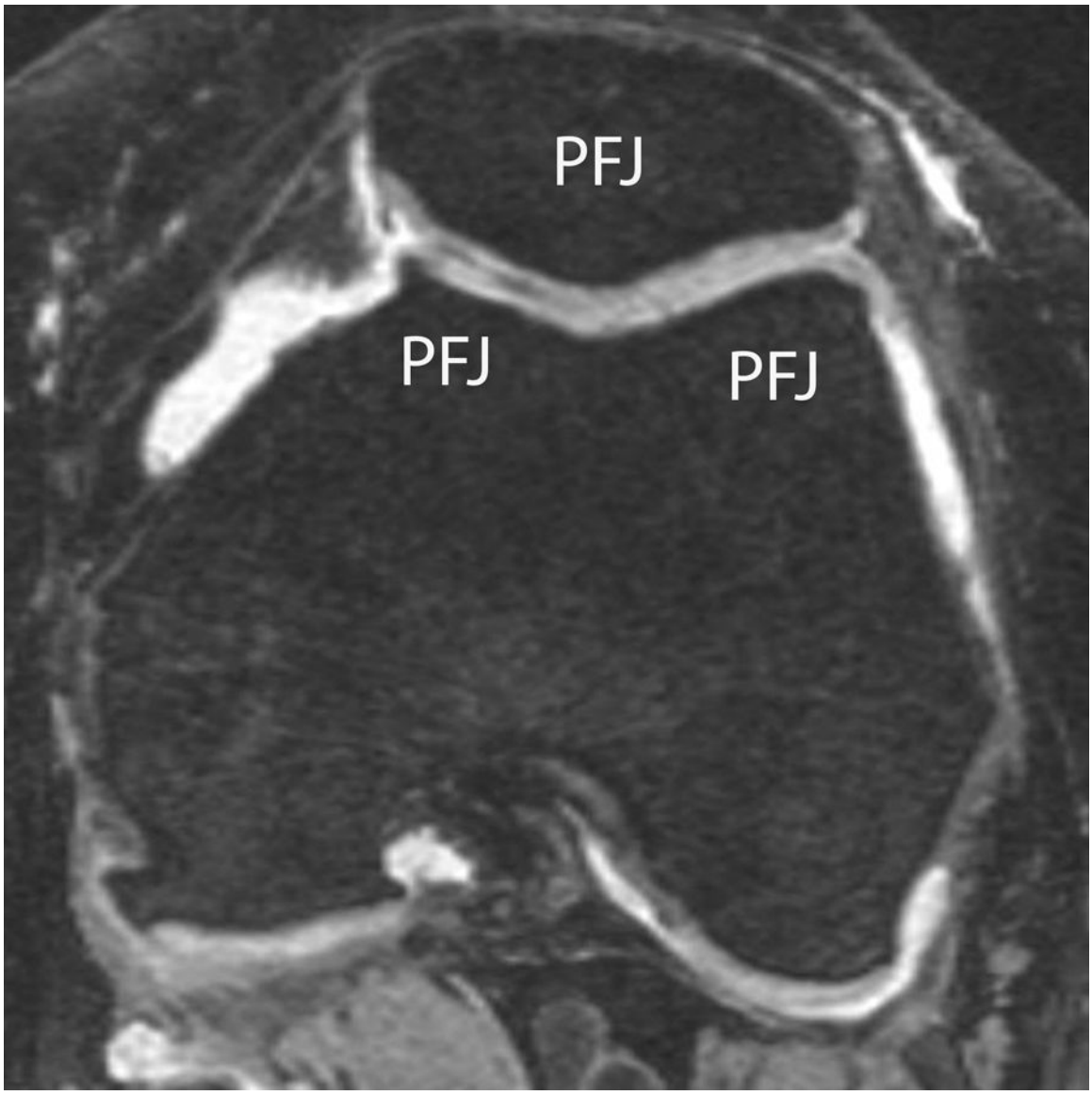

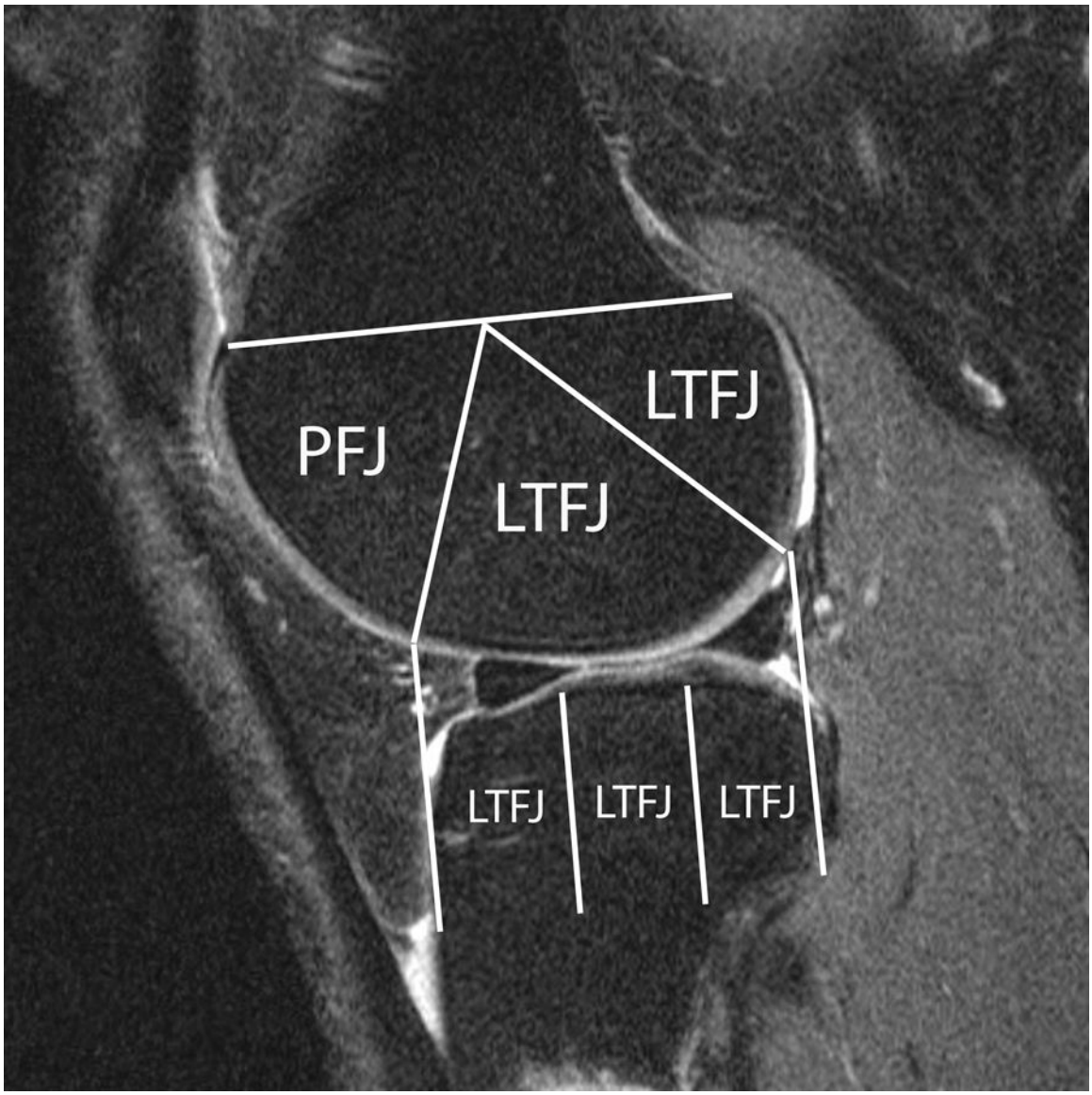

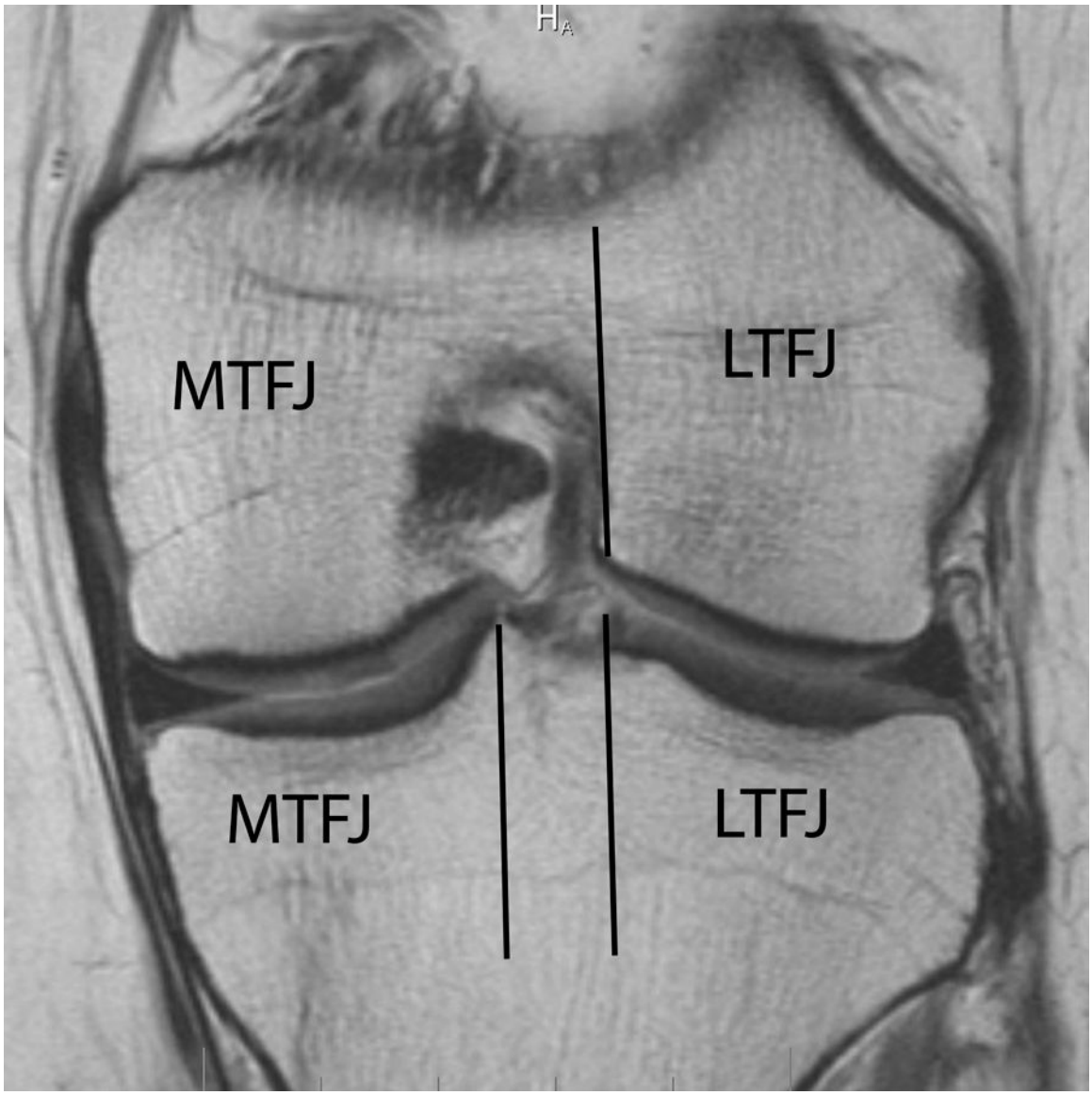

Figure 2.

Compartmental scoring approach in ROAMES. While subregions are defined in identical fashion as in MOAKS, only maximum grades per compartment are recorded. Only the maximum subregional scores of the patello-femoral, the medial and lateral tibio-femoral joints are considered. Figure depicts MOAKS subregions relabeled as compartmental categories as defined in ROAMES. A. Patello-femoral joint. The four MOAKS subregions of medial and lateral patella and the medial and lateral femoral trochlea are combined as patello-femoral joint. B. Sagittal intermediate-weighted fat suppressed image shows MOAKS subregions and assignment to the lateral tibio-femoral and the patello-femoral joints. C Coronal intermediate-weighted image shows the medial and lateral tibio-femoral compartments. Note that identical to MOAKS the femoral notch is part of the medial tibio-femoral joint.

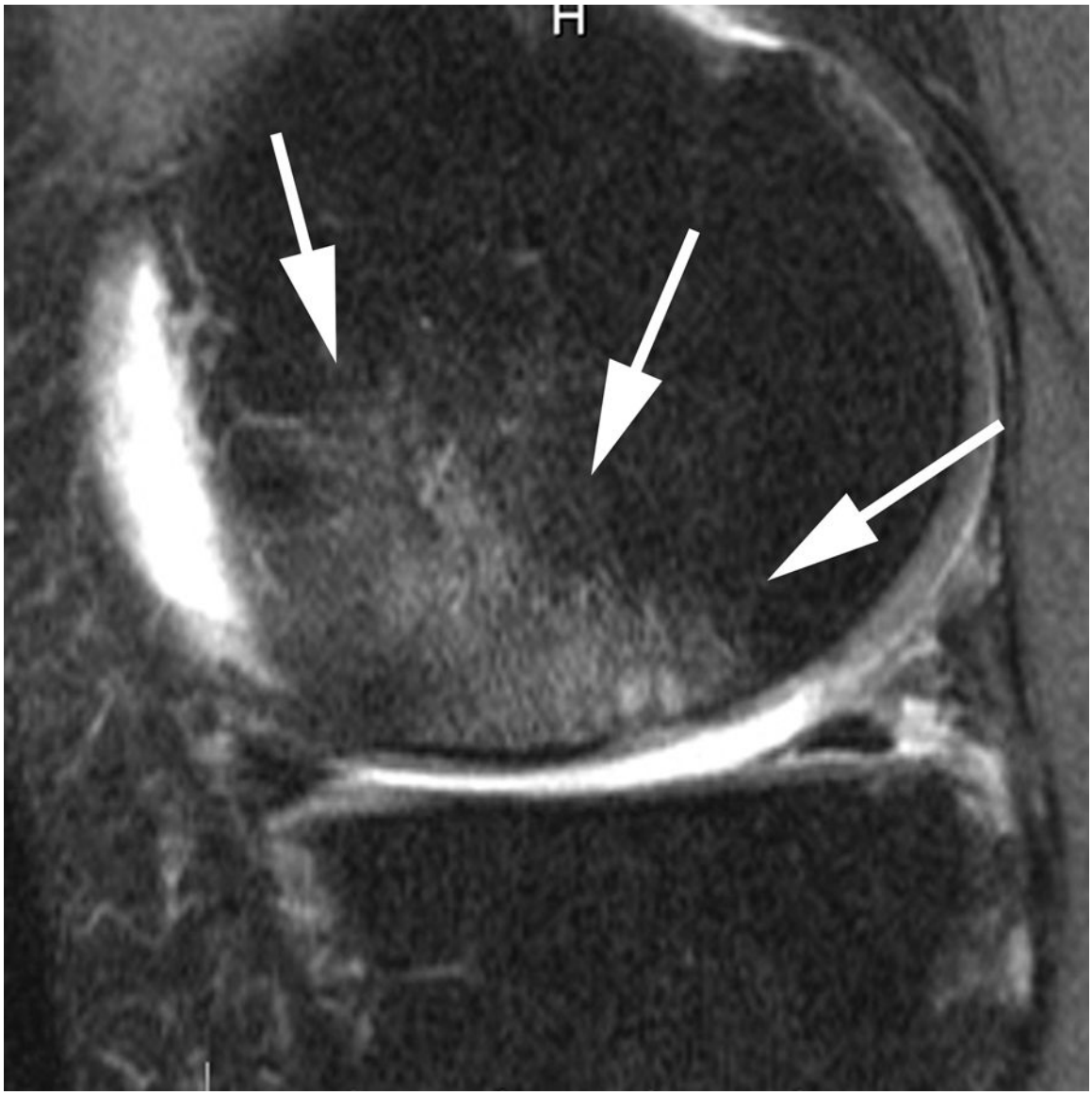

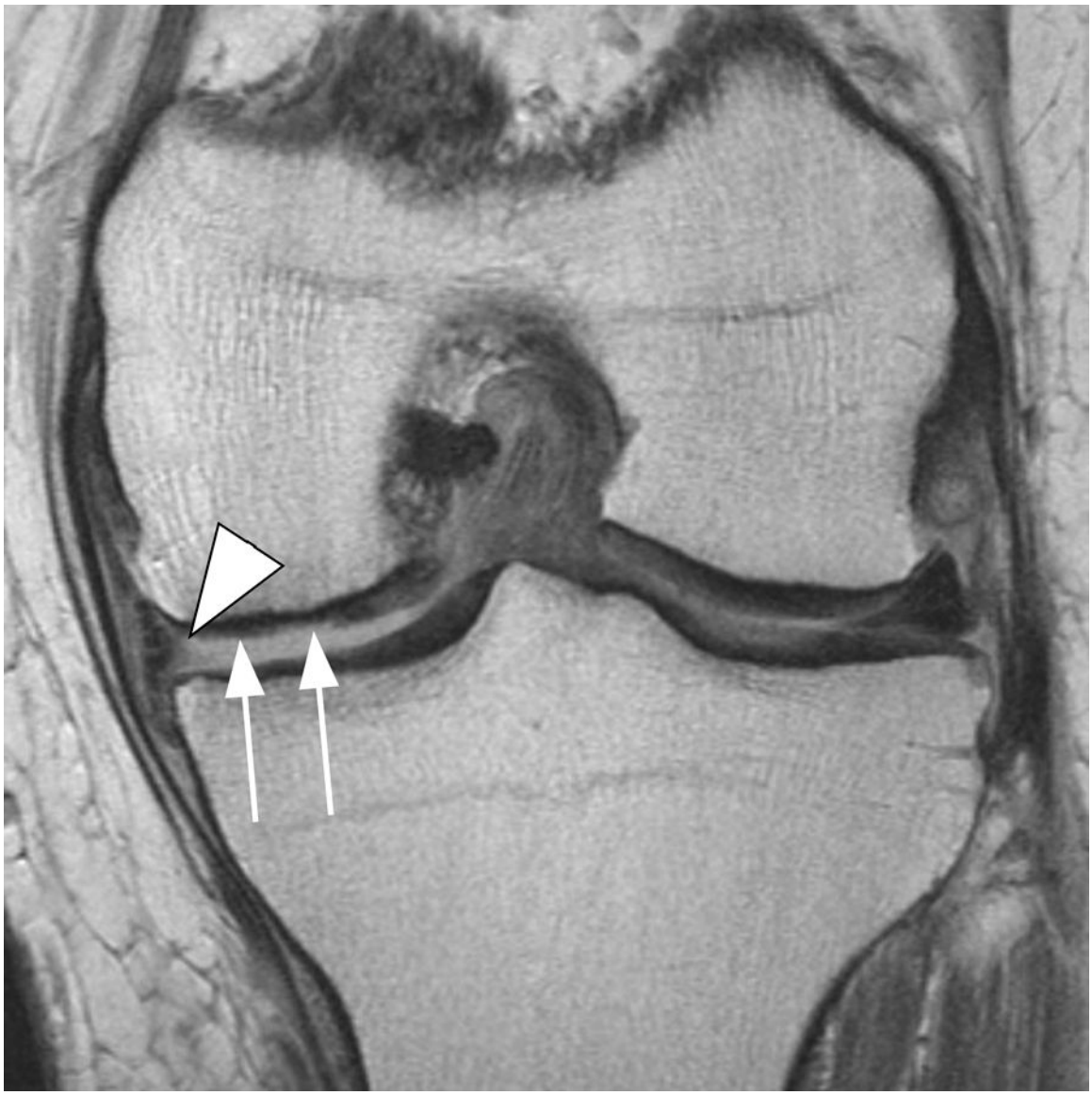

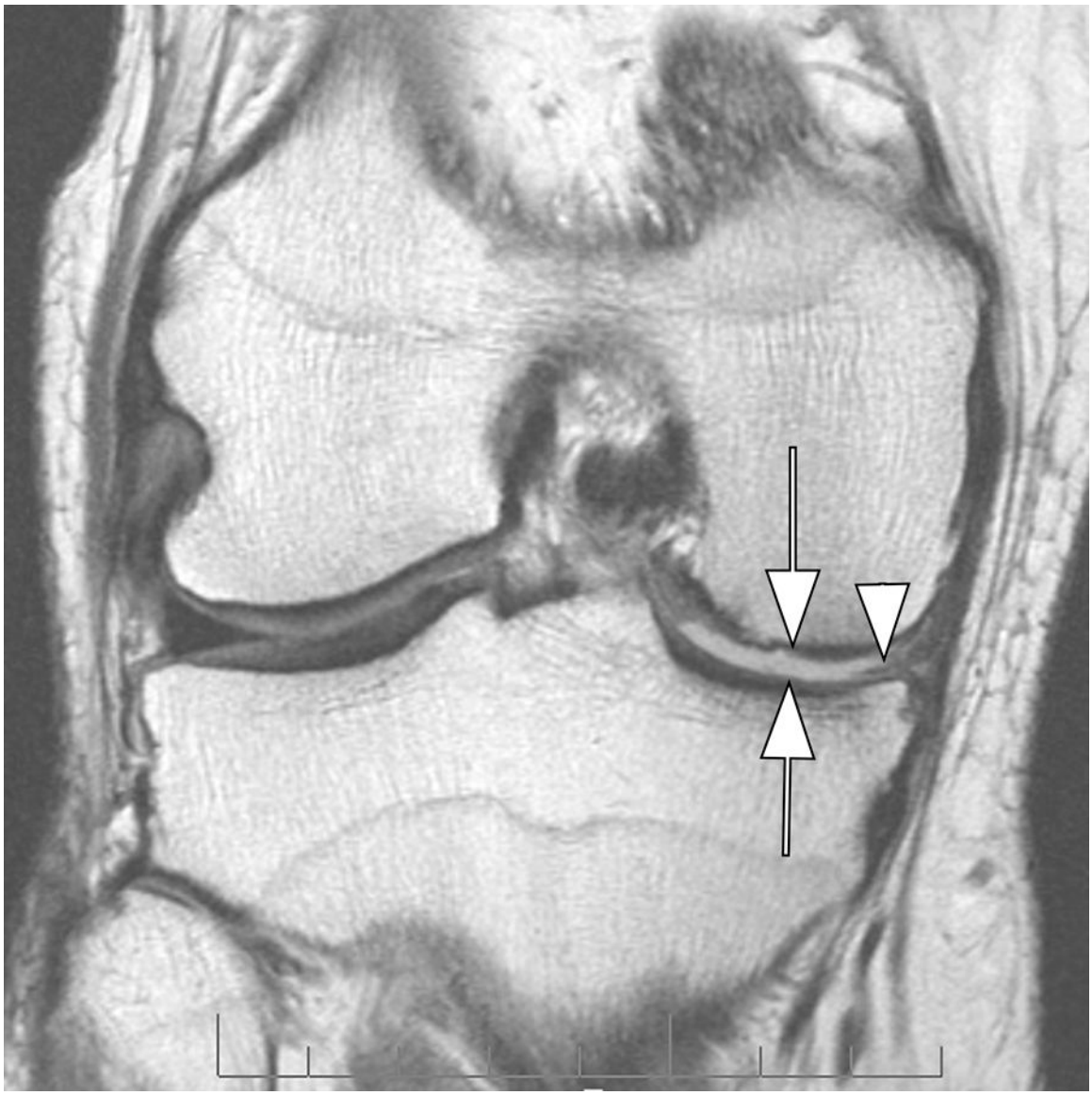

Figure 3.

Phenotypic characterization. A. The inflammatory phenotype is characterized by large joint effusion (asterisk) and so-called Hoffa-synovitis, a non-specific surrogate of whole knee synovitis. B. Bone phenotype. A large bone marrow lesion (BML) is present in the medial central subregion of the medial femur (grade 3, arrows). The maximum grade 3 BML defines this knee as a bone phenotype. C. The cartilage/meniscus phenotype is characterized by severe meniscal damage depicted in this example as partial meniscal maceration of the medial meniscal body (arrowhead) and commonly associated with severe cartilage loss (arrows point to diffuse superficial cartilage damage of the medial femur). In addition there is diffuse superficial cartilage damage at the medial tibia. D. The atrophic phenotype is characterized by severe cartilage loss without relevant osteophyte formation. There is marked cartilage damage in the medial compartment (arrows) and meniscal maceration (arrowhead) but no relevant osteophyte formation. This knee also fulfilled definition of the

cartilage/meniscus phenotype. E. The hypertrophic phenotype is characterized by large osteophytes with only minimal cartilage loss and is defined commonly in a compartmental manner. The arrow points to a grade 3 osteophyte according to ROAMES and a grade 2 osteophyte is depicted by the arrowhead at the medial tibia.

Table 1.

Identification of phenotypes by ROAMES and overlap between phenotypes

	Phenotypes (n)					
	Inflammatory	**Mechanical**	**Bone**	**Atrophic**	**Hypertrophic**	**Total N (%)**
Phenotype pre-defined by MOAKS	10	10	10	10	10	50 (100%)
Phenotype correctly identified by ROAMES	10	10	9	6	8	43 (86%)
Additional cases identified by ROAMES with same phenotype but not pre-defined	5 of 40 (12.5%) - 1 atrophic, - 1 mechanical, - 3 bone	2 of 40 (5%) - 1 inflammatory, - 1 bone	13 of 40 (32.5%) - 5 hypertrophic, - 2 atrophic, - 6 inflammatory	6 of 40 (15%) - 2 bone, - 3 mechanical, - 1 inflammatory - 2 inflammatory	2 of 40 (5%)	n/a
Number of additional phenotypes beyond pre-defined phenotype per knee						
No additional phenotype	3	7	4	8	5	27 (54%)
1 additional phenotype	4	2	6	1	5	18 (36%)
2 additional phenotypes	3	1	0	1	0	5 (10%)

Table 2.

Intra- and inter-observer agreement for ROAMES assessment

	Intra-Observer agreement		Inter-Observer agreement	
Feature and location	**Weighted Kappa (95% confidence interval)**	**% agreement**	**Weighted Kappa (95% confidence interval)**	**% agreement**
Cartilage PFJ	0.94 (0.85,1.00)	95.0	1.00 (1.00,1.00)	100.0
Cartilage medial TFJ	1.00 (1.00,1.00)	100.0	0.98 (0.93,1.00)	97.5
Cartilage lateral TFJ	1.00 (1.00,1.00)	100.0	0.92 (0.81,1.00)	95.0
BML PFJ	1.00 (1.00,1.00)	100.0	1.00 (1.00,1.00)	100.0
BML medial TFJ	1.00 (1.00,1.00)	100.0	0.98 (0.95,1.00)	97.5
BML lateral TFJ	0.94 (0.83,1.00)	97.5	0.89 (0.77,1.00)	95
Osteophytes PFJ	1.00 (1.00,1.00)	100.0	1.00 (1.00,1.00)	100
Osteophytes medial TFJ	1.00 (1.00,1.00)	100.0	0.95 (0.87,1.00)	95.0
Osteophytes lateral TFJ	0.95 (0.89,1.00)	95.0	0.95 (0.89,1.00)	95.0
Medial Meniscus	1.00 (1.00,1.00)	100.0	0.98 (0.95,1.00)	97.5
Lateral Meniscus	1.00 (1.00,1.00)	100.0	1.0000 (1.00,1.00)	100
Medial Meniscus Extrusion	0.96 (0.89,1.00)	95.0	0.96 (0.89,1.00)	95.0
Lateral Meniscus Extrusion	1.00 (1.00,1.00)	100.0	1.00 (1.00,1.00)	100
Hoffa Synovitis	0.92 (0.84,1.00)	92.5	0.85 (0.71,0.98)	87.5
Effusion Synovitis	0.94 (0.87,1.00)	92.5	0.92 (0.84,0.99)	90.0
Other findings[1]	1.00 (1.00,1.00)	100.0	1.00 (1.00,1.00)	100.0

Abbreviations: PFJ – patello-femoral joint; TFJ – tibio-femoral joint; BML – bone marrow lesion

[1]Other findings include most relevant structural diagnoses of exclusion: posterior meniscal root tear, subchondral insufficiency fracture, osteonecrosis, malignant bone marrow infiltration, traumatic fracture or bone contusion, solid tumors such as pigmented villo-nodular synovitis (PVNS, reclassified as diffuse-type giant cell tumor of the tendon sheath - dGCTTS – according to WHO 2013). Two cases were identified in the current dataset by both readers, one osteonecrosis and one PVNS.